Optimization of Diffractive MEMS for optical switching

J. Verheggen*, G. Panaman**, W. Khan Raja and J. Castracane

*College of Nanoscale Science and Engineering, University at Albany-SUNY, NFS-300 Suite 214, 255 Fuller Road, Albany, NY 12203, USA, jverheggen@uamail.albany.edu
**Currently at: DpiX, LLC, Palo Alto, CA, USA

ABSTRACT

Diffractive Micro-Electro-Mechanical Systems (D-MEMS) have enjoyed increased attention in the fields of communication, spectroscopy, projection display, and maskless lithography. The possible applications include: signal monitoring, signal attenuation, I/O reconfiguration, and add/drop multiplexing. Redirecting an optical signal into predefined angles, precisely balancing this optical signal, and its wavelength filtering capability is an advantage of D-MEMS over other optical MEMS. D-MEMS based on customized IC fabrication processes are being used to assemble system-level architectures for integration into mainstream circuitry. This paper focuses on an analysis of optimization parameters, summary of novel designs, experimental results, and polymer based D-MEMS fabrication.

Keywords: Diffractive MEMS, MOEMS, Diffraction gratings, Optical interconnect, Spectroscopy

1 INTRODUCTION

All-optical Dense Wavelength Division Multiplexing (DWDM) systems are being deployed in optical telecommunication networks because of the need for huge transmission bandwidth. Free Space Optical Interconnects (FSOI) at the microchip module level has been proclaimed as a possible solution to the electrical interconnect bottleneck that arises from ultra-high scale integration and increases in the maximum delay path. MEMS based active spectroscopy is investigated for lightweight, low power, active diffractive elements that are capable of achieving high spectral resolution for planetary spectroscopy, able to withstand vibrations during lift-off and operate in a radioactive environment.

2 DEVICE OPERATION

The MEMS Compound Grating (MCG) currently developed at the College of Nanoscale Science and Engineering (CNSE) consists of a grating whose rulings can be displaced perpendicular to the substrate. The original design consisted of a number of doubly clamped rulings. The active rulings are displaced by applying a potential between the rulings and the electrodes underneath. By displacing a set of rulings, the optical effect is to superimpose the interference patterns of several gratings, depending on the combination of rulings pulled down. This allows for a highly manipulative diffraction pattern.

This report focuses on a grating in which every other ruling is pulled down, and the grating period is twice the ruling length. When every other ruling is pulled down, the interference pattern of a grating with double the periodicity is superimposed on that of the original interference pattern. The passive diffraction pattern is that of a normal grating. Upon actuation, every other ruling is pulled down a quarter of the wavelength. This creates a diffraction pattern in which the original orders are extinguished and in between these orders, new orders arise, see Figure 1.[1]

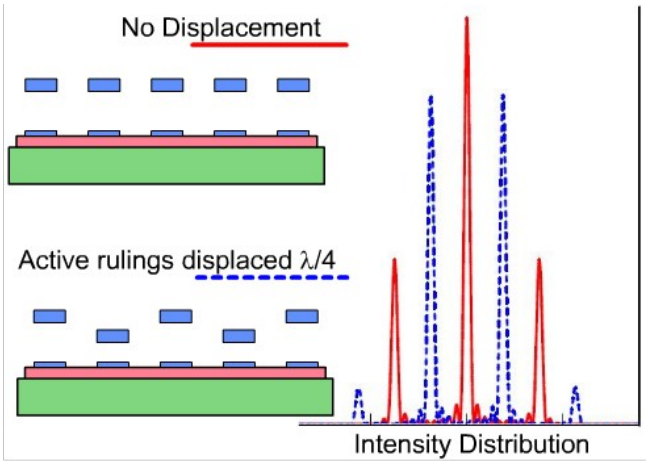

Figure 1: Cross section of MCG in passive state (upper left) and actuated state (lower left) and their corresponding diffraction patterns (right)

As can be seen from the diffraction pattern above, by displacing every other ruling λ/4, the original orders vanished, while new orders are at their maximum, resulting in switching of the optical signal. The angle of the diffracted orders as well as the displacement required for switching is wavelength sensitive, these properties make the MCG suitable for future optical networks as well as active spectroscopy.

3 DESIGN CONSIDERATIONS

To achieve commercialization in both the optical interconnect market as well as in planetary spectroscopy, certain parameters have to be optimized:

Switching at low voltage: devices manufactured at

CNSE have achieved switching of λ = 544nm light at 22V.[2] This potential should be reduced to below 5V. An important parameter for optical interconnects is switch speed. In order for reconfiguration of the I/O network, it is necessary to switch optically in the microsecond range. The insertion loss of every device should be reduced to a minimum. The spectral resolution defines the number of channels in an optical fiber. The current goal is to achieve 32 channels in a range of 1220 to 1620nm.

Switching voltage: In order to obtain a solid model for electro-mechanical behavior, the following differential equation is used in which *z(x)* is the displacement of the ruling along the *x*-axis, *g* is air gap, *b* is ruling width, *h* is ruling height, and $C_{1,2}$ are constants yet to be determined.

$$\frac{E\cdot b\cdot h^3}{12}\cdot\frac{d^4 z(x)}{dx^4}=\frac{\varepsilon\cdot b\cdot V^2}{2}\left(\frac{C_1}{(g+z(x))^2}+\frac{C_2}{b\cdot(g+z(x))}\right) \quad (1)$$

To include the fringe-field effect of the electrostatic force, an FEM simulation of the capacitance is obtained using Intellisuite™. The appropriate geometry of the two electrodes is imported: lower electrode is 0.5μm thick, upper electrode (ruling) is 1.5μm thick, both are 2μm wide. The imported structure is meshed with 0.2μm smallest mesh size. The capacitance at 5 different air gap values (2.75 - 1.65μm) are simulated. A function for capacitance is fitted through these values. The constants C_1 and C_2 are found to be 1.427 and 0.781 respectively. The electrostatic force including fringe field effect is then derived from this capacitance function. By utilizing the spring constant, a function can be derived that predicts operation voltage as function of center ruling displacement. This function is highly dependent on the applied boundary conditions, a doubly-pinned ruling is 5 times more flexible than a doubly-clamped ruling.

Device lifetime: This is dependent on the materials elastic behavior at low forces. Polysilicon has proven to be a very good elastic material.[3] The elastic behavior of the polysilicon MCG has previously been reported by this group.[1]

High switch speed: For steady state deflection a low spring constant is required. For fast switching speed, a high spring constant and high thickness (h) with small length (L) are required. See Equation (2) for natural frequency of doubly clamped ruling. These requirements are perpendicular to those for steady state deflection. In order to increase switch speed, while decreasing steady state operation voltage, the electrostatic force is increased by increasing capacitor area.

$$f_n=\frac{n^2\cdot\pi}{2L^2}\sqrt{\frac{E\cdot h^2}{12\cdot\rho}} \quad (2)$$

Insertion loss: This can be divided in three parts: material reflectance, fill factor, and diffracted order power. The first term can be increased by adding a gold layer on top of the polysilicon ruling which increases the reflectance from 28% to 95%. The second term is defined by the geometry of the device. The fill factor is ½ when the grating period is twice the ruling width. The third term is obtained by integrating the diffraction pattern between both minimums at each side of the diffracted order. Given a wavelength of 1550nm, the normalized diffracted power for orders 0 and 1 are 44.6% and 19.6%. At an active ruling displacement of λ/4, the normalized diffracted power for orders ½ and 1½ are 36.8% and 4.8% respectively. Half orders are the orders that arise in between the passive orders.

Spectral resolution: Spectral resolution for optical interconnects is dependent on the number of rulings illuminated (*N*) as described in Equation (3) where *m* is the diffraction order. This is equivalent for spectroscopy, but by producing a calibrated displacement of rulings, while registering the order intensity, one can perform coarse measurement of the wavelength. This feature can resolve the order-wavelength uncertainty, thereby eliminating the limitation of free spectral range typical of spectrometers based on conventional diffraction gratings. Another feature is the ability to identify a periodic function, which represents the "frequency" and "phase shift" of every diffraction order. For differential measurements of spectra, an angle of incidence can be found so that for any two adjacent orders the "phase shift" between them is 180^0.[4]

$$\lambda_2=\left(\frac{N+1/m}{N}\right)\cdot\lambda_1 \quad (3)$$

$$\varepsilon_C=\frac{h^2\cdot\pi^2}{12\cdot L^2} \quad (4)$$

The optical performance is optimal when both active and passive rulings are completely parallel. This parallelism is influenced by residual stress and ruling profile upon actuation. An important parameter for buckling is the critical Euler strain, Equation (4). It has been reported that this value between no buckling and buckling is not as profound and that its position and range are influenced by fabrication processes and design features. The critical strain does identify this transition region.[5]

4 FABRICATED DESIGNS

The original grating design consisting of a number of doubly-clamped rulings has some shortcomings. The ruling profile is altered upon actuation, reducing the effective optical area. In order to increase the steady state actuation deflection, the ruling length needs to be increased, which increases residual stress buckling and reduces the switch speed.

The cantilever designs introduce two flexible cantilevers at each end of a connected set of rulings. The ruling width is increased to 4μm to make room for passive rulings in between. While the anchors are 2μm wide, the ruling length

varies from 150 to 230µm. The connection between the rulings also increases the capacitive area. Three dimples are placed on the ruling to decrease the possibility of stiction. At the center of the ruling, this decreases the air gap from 2.75 to 2.10µm. Passive rulings are placed between the openings of the active frame. For certain designs, a gold layer is applied on top of the rulings to increase reflectivity. The second generation utilizes a T-shaped cantilever in order to obtain a more flexible anchor-cantilever interface.

In order to increase deflection while also increasing speed and optical performance, two new designs are introduced. These designs are manufactured by MEMSCAP using the PolyMUMPS process flow. The main goal of these devices was to increase parallelism of the active and passive rulings and to increase deflection by increasing capacitive area.

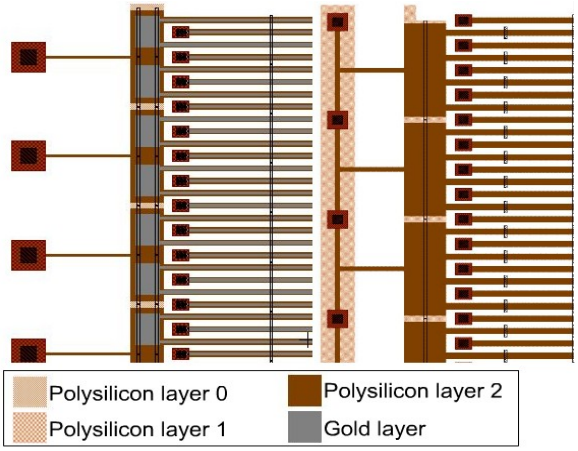

Figure 2: Cantilever design of 4 rulings grouped with straight cantilever (left) and T-shape cantilever plus gold layer on rulings (right)

The double grating design consists of two superimposed gratings with double periodicity, in which one is shifted a half period. Each grating occupies a different layer, the lower grating is displaced downwards while the upper frame is not moved. In one design, the lower frame is replaced by the electrodes on the substrate. The electrodes act as reflective grating as well as electrostatic actuators: the ruling width of these devices is 2µm, ruling length varies from 150 to 230µm.

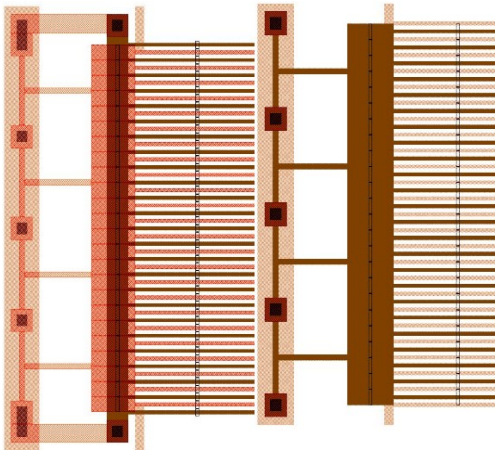

Figure 3: Double grating design: polySi 2 is active grating (left); PolySi 3 is active grating (right)

5 TEST RESULTS

The first generation of cantilever devices with gold on rulings showed high buckling behavior on SEM images. This was then verified using a white light interferometer, which showed buckling of ~1.3µm at the center of the ruling.[1] Optical experiments showed no switching at the center of the rulings, yet switching was observed at the ruling ends. Unbalanced residual stress of the gold and polySi layer led to non reproducible operation of these initial prototypes.

The first generation of cantilever designs without gold showed switching at 9.5V (Figure 4). A compact optical setup was constructed to test the device. The laser beam from a green He-Ne laser is spatially filtered with a pinhole, expanded and then collimated. A movable lens focuses this beam onto the MCG, allowing for spot size adjustment. A beam splitter was placed just before the MCG to allow for normal incident angle measurements. The diffraction pattern reflected back from the MCG is observed using a camera and optical profiler software.

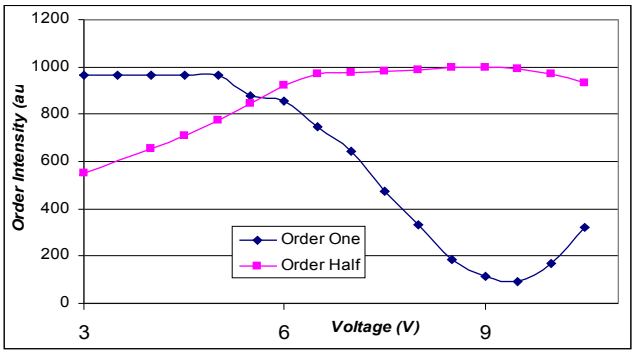

Figure 4: Order intensity as function of applied voltage for order 1 and ½ of cantilever design without gold.

The second generation cantilever, and the new double grating designs are fabricated and are undergoing interferometer testing as well as integration into technology demonstrator for optical interconnects.

6 POLYIMIDE FABRICATION

Through design changes, the actuation voltage has been reduced to under 10V. Of various techniques to lower the actuation voltage, a change in a material system with a lower Young's modulus is being investigated. The polysilicon devices that were fabricated through the MUMPS process have a Young's modulus of ~158 GPa[6]. Alternatively, polymers like polyimide and SU8 with much lower Young's modulus (~5GPa) are being considered as structural materials. The initial results from this approach showed a reduction of the actuation voltage to 8V for 544nm wavelength.[2]

The basic Polyimide MCG structure is identical to the 'original' designs and the layout was done using L-edit. The rulings were 4µm wide, with lengths of 130 to 200µm. Various ruling thicknesses will be investigated with varying air gap by process control. The mask set consisted of four chromium masks and the different layers were patterned on a contact aligner. The sacrificial layer is aluminum and photo-definable polyimide is used. A gold layer is deposited on the polyimide ruling for conductivity and reflectance.

The polyimide process flow is outlined in Figure 5 in which step 1 shows the Cr/Au/Ti bottom electrodes on SiO_2. An Al sacrificial layer is deposited and post holes are etched to the SiO_2. Step 3 shows the spin on of polyimide (HD-4002) which is then patterned and cured. Step 4 illustrates the deposition of Cr/Au as top electrode. The device is then released by etching the Al.

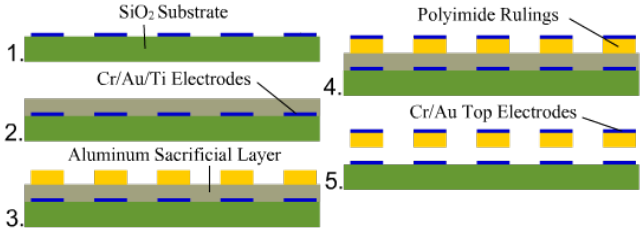

Figure 5: Process flow for polyimide based MEMS Compound Grating

6.1 Polyimide Processing

To obtain straight sidewalls, first a pre-bake analysis was performed, which resulted in cleared field with a pre-bake time of 180 sec. The exposure dose was determined by increasing the dose until it cleared the field. The 4 µm ruling width is close to the resolution limit and reflow during the post bake is a major issue. The effect of a post-bake is to lower the exposure dosage, and to increase adhesion. To decrease reflow of the polyimide sidewalls, the post-bake was omitted. The develop and rinse procedure consists of a three-beaker method in which first the wafer is placed in the developer, then placed in a developer rinse mix (1:1), followed by placing the wafer in the rinse beaker. A cross section of a developed polyimide grating is shown in Figure 6.

After development, the polyimide is cured at 375^0C. Photoresist is deposited and patterned after which a layer of Cr/Au is deposited on top of the polyimide rulings, which is patterned through liftoff. The reflow of polyimide in the cure process is problematic. It is countered by applying a plasma ash to clear the field. This last step needs to be optimized by varying the plasma energy. The device is released by etching Al using H_3PO_4, HNO_3, CH_3COOH, H_2O in 15:1:1:1 ratio.

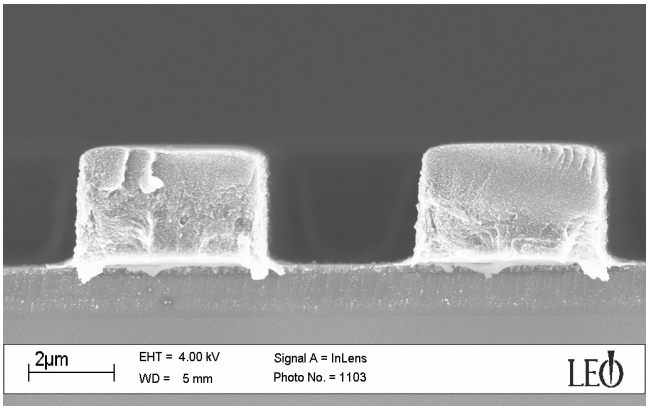

Figure 6: Cross section of developed polyimide grating on sacrificial Aluminum after development

7 CONCLUSION

Important aspects of MEMS compound grating devices are listed and investigated. Two new designs to optimize MCG performance are explained. These devices were fabricated and tested. The optical experiments have shown switching voltage of 544nm at 9.5V for the cantilever-based designs. The process flow of novel polyimide active gratings is provided. The final step of top electrode patterning is underway.

ACKNOWLEDGMENTS

The authors would like to thank Bruce Altemus and Larry Clow Jr. from CNSE for their help on polyimide processing and Stephen Kobak from ZYGO for his help in obtaining the white light interferometer data.

REFERENCES

1. J. Verheggen, G. Panaman, J. Castracane. Vol. 6114. p. 139-147. Proc: SPIE. (2006)
2. G. Panaman, S. Madison, M. Sano, and J. Castracane. Vol. 5719. p. 54-63. Proc: SPIE. (2005)
3. White Paper Silicon Light Machines, "*Breakthrough MEMS Component Technology for Optical Networks*", 2001 url <http://www.siliconlight.com/webpdf/>
4. J. Castracane, P. Schultz, M. Gutin, O. Gutin. Vol. . p. 1694. Proc: LPSC. (2000)
5. W. Fang, J. Wickert, Journal of Micromechanics and Microengineering, **4** (1994) 116-122, IOP
6. D. Koester, A. Cowen, R. Mahadevan, M. Stonefield, B. Hardy. *PolyMUMPs Design Handbook Rev. 10.0*. MEMSCap. 2003